J. Biochem. 2010;147(2):279–289 doi:10.1093/jb/mvp174

JB THE JOURNAL OF BIOCHEMISTRY

Expression and molecular characterization of the *Mycobacterium tuberculosis* PII protein

Received May 28, 2009; accepted October 6, 2009; published online November 2, 2009

Anannya Bandyopadhyay[1], Amit Arora[2], Sriyans Jain[1], Aparna Laskar[3], Chhabinath Mandal[3], Vladimir A. Ivanisenko[4], Eduard S. Fomin[4], Sergey S. Pintus[4], Nikolai A. Kolchanov[4], Souvik Maiti[2] and Srinivasan Ramachandran[1,*]

[1]Functional Genomics Unit, [2]Proteomics and Structural Biology Unit, Institute of Genomics and Integrative Biology (CSIR), Delhi 110 007, [3]Structural Biology & Bioinformatics Division, Indian Institute of Chemical Biology, 4 Raja S.C. Mullick Road, Kolkata 700 032, India and [4]Laboratory of Theoretical Genetics, Institute of Cytology and Genetics, Lavrentieva 10, Novosibirsk 630090, Russia

*Srinivasan Ramachandran, Functional Genomics Unit, Institute of Genomics and Integrative Biology, Near Jubilee Hall, Mall Road, Delhi 110 007, India. Tel: +91-11-2766-6156 ext.: 169; Fax: +91-11-2766-7471, E-mail: ramuigib@gmail.com; ramu@igib.res.in

The signal transduction protein PII plays an important role in cellular nitrogen assimilation and regulation. The molecular characteristics of the *Mycobacterium tuberculosis* PII (Mtb PII) were investigated using biophysical experiments. The Mtb PII coding ORF *Rv2919c* was cloned and expressed in *Escherichia coli*. The binding characteristics of the purified protein with ATP and ADP were investigated using surface plasmon resonance (SPR) and isothermal titration calorimetry (ITC). Mtb PII binds to ATP strongly with K_d in the range 1.93–6.44 μM. This binding strength was not significantly affected by the presence of 2-ketoglutarate even in molar concentrations of 66 (ITC) or 636 (SPR) fold excess of protein concentration. However, an additional enthalpy of 0.3 kcal/mol was released in presence of 2-ketoglutarate. Binding of Mtb PII to ADP was weaker by an order of magnitude. Binding of ATP and 2-ketoglutarate were analysed by docking studies on the Mtb PII crystal structure (PDB id 3BZQ). We observed that hydrogen bonds involving the γ-phosphate of ATP contribute to enhanced binding of ATP compared with ADP. Glutaraldehyde crosslinking showed that Mtb PII exists in homotrimeric state which is consistent with other PII proteins. Phylogenetic analysis showed that Mtb PII consistently grouped with other actinobacterial PII proteins.

Keywords: Nitrogen metabolism/Calorimetry/Surface plasmon resonance/Bacteria/Nucleotide binding.

Abbreviations: IPTG, isopropyl-D-thio-β-galactopyranoside; ITC, isothermal titration calorimetry; Mtb, *Mycobacterium tuberculosis*; Ni–NTA, nickel–nitrilotriacetate; SPR, surface plasmon resonance.

Tuberculosis caused by *Mycobacterium tuberculosis* is still a major killer infectious disease worldwide. This problem is compounded by the emergence of multi-drug-resistant strains of *M. tuberculosis* and the poor efficacy of the currently available vaccines (*1*, *2*). Therefore, there is an urgent need to develop new strategies including identification of drug targets and of potential vaccine candidates. A necessary pre-requisite step towards accomplishing this goal is the molecular characterization of the genes and their product proteins (*1*).

The signal transduction protein PII plays an important role in cellular nitrogen assimilation and regulation (*3*). The *PII* gene is very widely distributed and is highly conserved, with homologues in archaea, bacteria and eukaryotes (*3*). The protein PII integrates the antagonistic signals of status of intracellular carbon and nitrogen and uses this information to control nitrogen assimilation (*4*).

Characterization of PII (GlnB) protein from enterobacteria showed that it is a homotrimeric protein. It functions at the interface of signal sensing and regulation of primary nitrogen assimilation through the glutamine synthetase–glutamine 2-ketoglutarate aminotransferase (GS/GOGAT) cycle (*5*). This is accomplished in two ways: (i) through uridylylation of PII in response to the levels of the nitrogen-status signal molecule glutamine and (ii) the allosteric binding of the carbon status indicator molecule 2-ketoglutarate (*6*, *7*).

Depending on the uridylylation status, PII controls the activity of glutamine synthetase in the form of regulating the expression of the GS gene *glnA*1 via the NtrB–NtrC (two component system) and transduction of cellular nitrogen status to adenylyltransferase (*8*, *9*).

Interestingly, a second PII protein termed GlnK has also been identified in *Escherichia coli* (*10*). The amino acid sequence of *E. coli* GlnK bears 67% identity to the *E. coli* GlnB sequence, and the protein is encoded in an operon with a second downstream gene *amtB*, which encodes for an ammonium transporter (*10*). GlnK can also be post-translationally modified by uridylylation at the tyrosine 51 residue and has been shown to bind and regulate the activity of AmtB (*11*, *12*). The presence of two or more than two PII-like proteins has been reported in many other proteobacteria (*13*, *14*). In *Rhodospirillum rubrum*, three paralogues of PII have been identified, namely, GlnB, GlnJ and GlnK (*15*).

In contrast to proteobacteria, the presence of additional *glnB*-like genes have not been reported in either cyanobacteria or gram positive bacteria so far (*3*). In case of actinomycetes, only a single gene encoding PII has been identified (*16*–*18*). It has been shown that

GlnK is essential for adaptation of *Corynebacterium glutamicum* to nitrogen starvation (*16*).

M. tuberculosis has a single gene (*Rv2919c*) encoding the PII protein (Mtb PII). The gene *Rv2919c* is annotated as *glnB* in Tuberculist (*19*). The Mtb PII sequence bears 61.1% identity to *E. coli* GlnB and 54% identity to *E. coli* GlnK sequences, indicating its probable orthologous relationship with GlnB. However, according to Arcondeguy *et al.* (*3*), the Mtb PII is likely GlnK on the basis of gene neighbourhood analysis. In this communication, we report the molecular characterization of Mtb PII. The gene encoding Mtb PII has been cloned, over-expressed and purified. The trimeric status of the protein was observed by chemical cross-linking. Binding characteristics of ATP and ADP were determined using surface plasmon resonance (SPR) and isothermal titration calorimetry (ITC). Docking analysis with the published crystal structure was used to gain insights into the binding characteristics of ATP, ADP and 2-ketoglutarate.

Materials and methods

Polymerase chain reaction (PCR) amplification and cloning of MtbPII gene (Rv2919c)

Mtb PII was cloned in pET28a(+) for expression as an N-terminal his-tagged protein. *M. tuberculosis* H37Rv genomic DNA was used as the template for PCR amplification. The sequence of the forward primer was 5′-AGT GGA GGC **GGA TCC** GAA ATG AAG CTG ATC-3′, and that of the reverse primer was 5′-AGC ACA GTG **AAG CTT** GTT TCA TAA CGC GTC GTG-3′. The sites for restriction enzymes *BamHI* and *HindIII* were added before the start codon ATG in the forward primer and after the stop codon in the reverse primer, respectively. The PCR conditions were: initial step of one cycle of 5 min at 95°C followed by 25 cycles of 1 min at 95°C, 45 s at 64°C, 1 min at 72°C and a final step of one cycle of 10 min at 72°C, using *Taq* DNA polymerase (Bangalore Genei, India). The resulting 375 bp amplified PCR product was electrophoresed through a 1% Agarose gel (USB, USA). The desired DNA band was cut in the gel and purified using DNA isolation kit (Biological Industries, Israel). PCR product was sequentially digested with the restriction enzymes *BamHI* and *HindIII* and then cloned in frame into pET28a(+) (Novagen, USA) predigested with the same restriction endonucleases. The fusion construct coded for an N-terminal hexa histidine tagged recombinant Mtb PII. Sequencing of the clone revealed a non-synonymous codon change (T→P) at the fifth codon and a synonymous codon change at 79th codon. However, the ATP-binding site, the T-loop sequences were identical to that given in Tuberculist for *Rv2919c*.

Mtb PII was also cloned in pET23b vector for expression as a C-terminal his-tagged protein. PII coding region was amplified by PCR using forward primer (5′-GGA GG**G AAT TCC** GAA ATG AAG CTG ATC ACT-3′, and reverse primer (5′-ACA GTG CGG CTA **AAG CTT** TAA CGC GTC GTG-3′) containing *EcoRI* and *HindIII* recognition sites, respectively. After digestion with *EcoRI* and *HindIII*, the PCR product was cloned into *EcoRI–HindIII*-restricted pET23b vector (Novagen, USA) to produce a C-terminal hexa-histidine tagged Mtb PII. Sequencing revealed complete identity to Tuberculist sequence for *Rv2919c*.

Over-expression and purification of recombinant N- and C-terminal his-tagged MtbPII

The N-terminal his-tagged fusion construct was transformed into *E. coli* rosetta strain (Novagen, USA). The transformed cells were grown at 37°C in Luria Broth containing 50 μg/ml Kanamycin and 34 μg/ml Chloramphenicol. At an optical density at 600 nm (OD_{600}) of 0.6, expression of recombinant protein was induced by adding isopropyl-D-thio-β-galactopyranoside (IPTG; Sigma, USA) to a final concentration of 0.2 mM and incubation was continued for 3 h with vigorous shaking (230 rpm). Cells (250 ml culture) were harvested by centrifugation at 6800 × *g* at 4°C and the cell pellet was resuspended in 10 ml of lysis buffer [20 mM Tris–HCl, pH 7.9, 1.25 M NaCl, 5 mM imidazole, 1 mM phenyl methyl sulfonyl fluoride (PMSF; Sigma, USA)]. Cells were lysed by sonication (Mesonix XL3000, USA) with 30 cycles of 30 s pulse and 20 s rest on ice and the sonicated cell suspension was centrifuged at 29 000 × *g* for 30 min at 4°C. Expressed protein was found to be soluble by analyzing supernatant and pellet fractions on SDS–PAGE (12%) (*20*). Purification of his-tagged Mtb PII was carried out by affinity chromatography on nickel–nitrilotriacetate (Ni–NTA) resin column (Qiagen, Germany). The soluble fraction was incubated with 1 ml of Ni–NTA resin pre-equilibrated with equilibration buffer (20 mM Tris–HCl, pH 7.9, 500 mM NaCl) for 2 h at 4°C. The supernatant was loaded onto the column and washed with 10 column volumes of wash buffer-1 (20 mM Tris–HCl, pH 7.9, 500 mM NaCl, 5 mM imidazole), 25 column volumes of wash buffer-2 (20 mM Tris–HCl, pH 7.9, 500 mM NaCl, 20 mM imidazole), five column volumes of wash buffer-3 (20 mM Tris–HCl, pH 7.9, 500 mM NaCl, 50 mM imidazole) and five column volumes of wash buffer-4 (20 mM Tris–HCl, pH 7.9, 500 mM NaCl, 100 mM imidazole). Bound protein was eluted with 15 column volumes of elution buffer (20 mM Tris–HCl, pH 7.9, 500 mM NaCl, 300 mM imidazole). Fractions containing significant amounts of PII, as judged by SDS–PAGE (12%) analysis were pooled and then concentrated to 250 μg/ml using Amicon Ultra-15 (5 K NMWL) concentrator (Millipore, USA), and stored at 4°C. Concentration of protein was detected by the Bradford method (*21*) using BSA (Sigma, USA) as standard.

The C-terminal his-tagged fusion construct was transformed into *E. coli* C41 strain (Avidis, France). Protein expression and purification protocol was similar to that of N-terminal his-tag Mtb PII described above, with minor changes. Protein expression was induced with 1 mM IPTG. Freshly prepared lysozyme was added to the cell suspension (1 mg/ml) ahead of cell lysis by sonication. The column bound Mtb PII-C protein (C-terminal 6XHis tag) was washed with three wash buffers containing 5, 20 and 60 mM imidazole. Bound protein was eluted with elution buffer containing 150 mM imidazole. Fractions containing significant amounts of PII, as judged by SDS–PAGE (12%) analysis were pooled, concentrated and stored at 4°C.

Purified recombinant Mtb PII was confirmed by peptide mass fingerprinting using MALDI-TOF mass spectrometry. For protein identification, the peptide mass list acquired after trypsin digestion of the protein was searched against mass spectrometry database (MSDB) using the MASCOT search engine (Matrix Science, UK, using BioTools™ 2.2 software).

Circular Dichroism Spectroscopy

A Chirascan (Applied Photophysics) circular dichroism spectrophotometer was used to measure the ellipticity of purified recombinant N-terminal his-tagged Mtb PII protein at 0.08 mg/ml in HEPES-buffered saline {5 mM HEPES [*N*-(2-hydroxyethyl)piperazine-*N*′-(2-ethanesulfonic acid)], pH 8.0, 100 mM NaCl} from 10 to 70°C with intervals of 5°C. Each spectrum, recorded at 1 nm intervals using a 0.1 cm path length cuvette, was taken in the far-UV region from 190 to 250 nm and averaged over three scans. The recorded spectra in millidegrees of ellipticity were converted to molar ellipticity (θ) in deg. cm^2 $dmol^{-1}$ Molar ellipticity of the protein at 225 nm wavelength was plotted as a function of temperature to ascertain the thermal stability of the protein.

Biacore SPR Analysis

The binding characteristics of ATP and ADP to Mtb PII protein were studied by SPR analysis using a Biacore® 2000 instrument (Biacore, Sweden) at 25°C. Carboxymethylated dextran chip (sensor chip CM5, research grade, Biacore AB, Sweden) was used in the assay. The protein sample to be coupled was diluted in 10 mM sodium acetate buffer (pH 5.0) to achieve a net positive charge for amine coupling. The activation step was performed with 60 μl of freshly prepared 1:1 solution of 100 mM *N*-hydroxysuccinimide and 400 mM *N*-ethyl-*N*′-(dimethylaminopropyl)-carbodiimide (3 min at 20 μl/min). Purified recombinant Mtb PII of the quantity 25 μg/ml (1.57 μM) was injected at the rate of 2 μl/min to attain 4500 resonance units (RU), an appropriate level of coupling for the binding experiments. The flow cell surfaces were then deactivated with 40 μl of 1 M ethanolamine–HCl (pH 8.5) at the rate of 20 μl/min.

HBS (HEPES-buffered saline, 20 mM HEPES, 5 mM $MgCl_2$, 100 mM NaCl, 0.005% Nonidet P40, pH 8.0) either with 2-ketoglutarate (1 mM, in case of ATP only) or without 2-ketoglutarate, was used as the continuous running buffer during the experiments. All buffers were degassed. For the binding studies of ATP and ADP, 100 µl of various concentrations of the nucleotide triphosphate or diphosphate (10, 20, 40, 80, 160, 320 and 640 µM), dissolved in the running buffer, was injected through both the flow cell (with the coupled protein) and control flow cell (a parallel flow cell, which was activated and then deactivated without any coupled protein) simultaneously at a flow rate of 20 µl/min at 25°C. The dissociation phase, initiated by the passage of HBS alone, was carried out over a period of 5 min. The biosensor surfaces were regenerated by a 2 min injection of 500 mM NaCl. Samples were injected in duplicate and in random order.

Sensorgrams were analysed with BIAevaluation 3.1 software (Biacore AB, Sweden). To correct the refractive index changes, the responses generated in the control surface were subtracted from the responses generated in the surface with immobilized protein. The binding data from the injection of different concentrations of ATP and ADP were globally fitted to a 1:1 Langmuir binding model. Statistical significance of differences in comparisons between the average values of the association and dissociation rate constants (k_a and k_d, respectively) were examined by the criterion: if average k_a (or k_d) of one nucleotide was greater or lesser than that of another nucleotide ± 3 standard error (SE) of fitting, then the difference between average k_a (or k_d) was taken as statistically significant.

ITC analysis

The values of thermodynamic variables governing binding of ATP and ADP to the purified recombinant Mtb PII protein were characterized by ITC using a VP-isothermal titration calorimeter from MicroCal, Inc (USA). A purified preparation of the protein was dialysed extensively for 18 h against ITC buffer (20 mM Tris–HCl pH 7.9, 150 mM NaCl) and degassed prior to use. The nucleotide triphosphates and diphosphate solutions were prepared in ITC buffer with 5 mM $MgCl_2$. All titrations were performed at 30°C using a syringe while stirring continuously at 300 rpm. For determination of ATP and ADP-binding isotherms, the protein solution (12–15 µM protein in ITC buffer) was titrated with 15–30 additions of nucleotide solution (5 µl of 1 mM each). Each injection of nucleotide lasted 5 s with 5 min interval between successive injections. For determining the binding of ATP in the presence of 2-ketoglutarate, the ATP solution injections were carried out in the presence of excess of 2-ketoglutarate (1 mM). All experiments were repeated three times with the same instrument settings.

Enthalpies of binding were determined by integrating the signals from the calorimeter. The heats of dilution of the ligand for each experiment were measured separately in a similar experiment in which the solution in the calorimeter cell was devoid of protein. The binding isotherm was generated by plotting the corrected heats of binding against the ratio of ligand to protein. The enthalpy change (ΔH) and the binding constant (K_a) were directly obtainable from the experiments after processing the data using Origin software, Version 7.0 (MicroCal, USA). The dissociation constant (K_d), Gibbs free energy (ΔG°) and entropy (ΔS) were subsequently calculated using $K_d = 1/K_a$, $\Delta G^\circ = -RT \ln K_a$ and $T\Delta S = \Delta H - \Delta G$, respectively. Welch two sample *t*-tests for assessing the statistical significant difference in means of these thermodynamic quantities from triplicate experiments were carried out using R (ver 2.4.0) package (*22*), for the ΔH, ΔG, ΔS and K_a values obtained for the nucleotides.

ATP and 2-ketoglutarate docking study

The crystal structure of Mtb PII (PDB id 3BZQ) was taken from the Protein Data Bank (*23*). ATP-binding site in the PII crystal structure was predicted by PDBSiteScan software (*24*, *25*). Optimization of the complex and docking analysis was performed using MOLKERN and AUTODOCK softwares (*26*, *27*). For modeling the structure in presence of 2-ketoglutarate (IUPAC name: 2-oxopentanedioic acid) the 3D structure of PII peptide chain with bended T-loop was modelled by SWISS-MODEL server (*28*) using *Methanococcus jannaschii* PII structure (PDB id 2J9E) as template (*29*). The complex of 2-ketoglutarate with the modelled monomer of the Mtb PII was predicted and the structure of the complex was obtained by the PDBSiteScan software (*24*, *25*) In the next step, optimization of the complex and docking analysis was performed using MOLKERN and AUTODOCK softwares (*26*, *27*).

Glutaraldehyde crosslinking reaction

Crosslinking reaction was performed to stabilize the oligomer form of the protein which can be distinguished from the monomer form following SDS–PAGE analysis. Glutaraldehyde was chosen for chemical cross-linking for reasons that included aqueous solubility, homobifunctional specificity for lysine residues, short spacer length (5 Å) (*30*). A typical reaction contained 5 µg (0.33 µmoles) PII-C protein suspended in 50 µl of 20 mM HEPES, pH 7.9, 150 mM NaCl. Glutaraldehyde concentration was varied from 0.5 to 10%. The samples were incubated at 37°C for 4 h. Reactions were terminated by addition of 6 µl of 1 M Tris–HCl, pH 7.9. Samples were electrophoresed on SDS–PAGE (12%).

Molecular phylogenetic analysis

Amino acid sequences of PII orthologs from several species were aligned using ClustalW program with default parameters (*31*). Two sets of experimentally studied PII protein GlnB and GlnK sequences from proteobacteria were selected. We chose two sets because according to Tuberculist (*19*), the Mtb PII is a GlnB homolog but according to Arcondeguy *et al.* (*3*) it may be GlnK homolog. Probable PII protein sequences from species of the Mycobacterial family were selected along with *S. coelicolor* and *C. glutamicum* PII sequences from the rest of the actinomycete group. The following amino acid sequences were selected: *M. tuberculosis* (*Mycobacterium tuberculosis* H37Rv, GI:15610056), *M. bovis* (*Mycobacterium bovis* AF2122/97, GI:31794095), *M. avium* (*Mycobacterium avium* subsp. Paratuberculosis BAA-968/K-10, GI:41409085), *M. smegmatis* (*Mycobacterium smegmatis* MC2, GI:118172186), *C. glutamicum* (*Corynebacterium glutamicum* ATCC 13032, GI:19553261), *S. coelicolor* [*Streptomyces coelicolor* A3(*2*), GI:32141267], *E. coli* [*Escherichia coli* K-12, (GlnB, GI:16130478), (GlnK, GI:16128435)], *N. meningitidis* [*Neisseria meningitidis* MC58, GlnB, GI:7227257], *K. pneumoniae* [*Klebsiella pneumoniae*, (GlnB, GI:43806), (GlnK, GI:3954959)], *A. brasilense* [*Azospirillum brasilense*, (GlnB, GI:12698724)], *Azoarcus* [*Azoarcus* sp. BH72, (GlnB, GI:11761787), (GlnK, GI:11761785)], *R. palustris* [*Rhodopseudomonas palustris* CGA 009, (GlnB, GI:24473719), (GlnK1, GI:39652974), (GlnK2, GI:39652976)].

The PHYLIP version 3.6 was used for the phylogenetic analyses (*32*). Pair wise sequence distances were estimated using Henikoff/Tillier PMB matrix (*33*) in the Protdist program. The Fitch program was used for construction of the trees (*34*, *35*). The unrooted trees were plotted using the Drawtree program. Bootstrap analyses (1000 replicates) were performed for both trees using Seqboot program (*36*). Consensus trees were obtained using Consense program.

Results

Cloning, expression and purification of recombinant Mtb PII protein

The purified N-terminal his-tagged Mtb PII protein was identified as a 16 kDa band on SDS–PAGE (12%) and was observed to be of >95% purity as determined by SDS–PAGE. About 2.5 mg of purified PII was obtained per liter of induced *E. coli* culture. The protein was stable at pH 7.9 in Tris–HCl and HEPES buffers and were stored at 4°C. The purified protein was confirmed to be Mtb PII by peptide mass fingerprinting using MALDI-TOF mass spectrometry.

Circular dichroism

In order to carry out PII interaction studies with small molecules, it was important to determine the presence of ordered structure of the purified protein at 25 and 30°C. Therefore, we used CD spectroscopy to examine the presence of secondary structure in Mtb PII. Far-UV CD spectra at both temperatures were similar

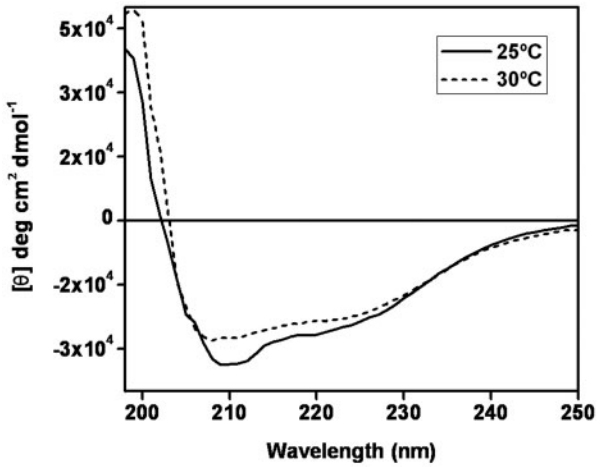

Fig. 1 Circular dichroism spectroscopy of Mtb PII. The far-UV CD spectra of purified PII (0.08 mg/ml in 5 mM HEPES, pH 8.0, 100 mM NaCl) at 25 and 30°C.

but with minor change in ellipticity (Fig. 1). We observed that the slight change in CD spectra is consistent in both buffers (5 mM HEPES, pH 8.0, 100 mM NaCl and 10 mM KH_2PO_4, K_2HPO_4, pH 8.0, 100 mM NaCl). The molar ellipticity values at 225 nm changed to an extent of 5.5%. This indicated slight structural change. This observation prompted us to examine the temperature effects on the protein over a long range from 10 to 70°C. The experiment was carried out in both HEPES and potassium phosphate buffers. A sigmoid curve was observed between molar ellipticity at 225 nm and the temperature. It was evident that even at 70°C the protein retained significant fraction of secondary structure, $[\theta]_{225,\,70^\circ C} = -1.37 \times 10^4\,\mathrm{deg\,cm^2\,dmol^{-1}}$. These observations indicated only a partial loss of structure. In comparison, the structural change in the protein shown by change in molar ellipticity at 25°C ($-2.36 \times 10^4\,\mathrm{deg\,cm^2\,dmol^{-1}}$) and 30°C ($-2.23 \times 10^4\,\mathrm{deg\,cm^2\,dmol^{-1}}$) is minor (5.5%) (Supplementary Figure S1).

Surface plasmon resonance analysis

The binding characteristics of ATP and ADP to Mtb PII protein were analysed by SPR. The results are displayed in Fig. 2. The SPR measurements showed that binding of nucleotides to Mtb PII were reversible. Kinetic rate constants were determined by globally fitting the data to a 1 : 1 Langmuir binding model. This showed that on an average each subunit of PII protein binds to one nucleotide molecule.

The association and dissociation rates of Mtb PII–ATP and PII–ADP complexes are displayed in Table 1. The association rate for the formation of PII–ATP complex was higher than that of ADP. In the presence of 1 mM 2-ketoglutarate, the association and dissociation rates of Mtb PII–ATP complex were significantly lower than in the absence of 2-ketoglutarate (Table 1). ADP showed significantly lower association and dissociation rates. Association rate constant for the formation of PII–ADP complex was 6.8-folds significantly lower than ATP and the

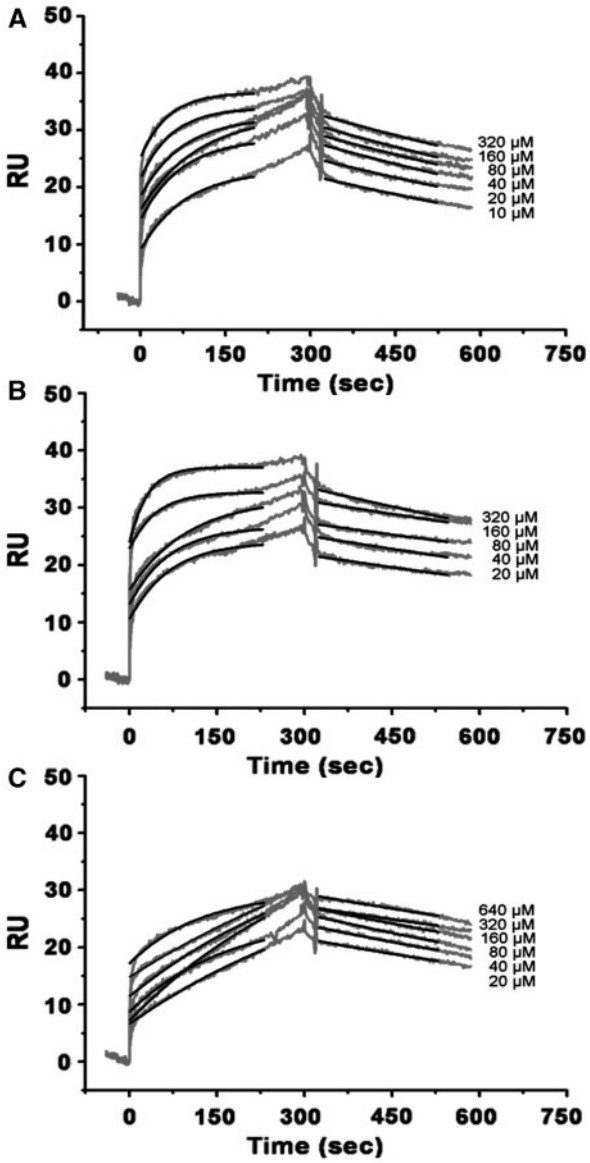

Fig. 2 Analyses of Mtb PII binding to nucleotides by surface plasmon resonance. The sensorgrams show the relative response for interactions between immobilized PII when nucleotides were injected at varied concentrations (10–640 µM). Each injection concentration was repeated twice in random order. Both experiments were carried out in the presence of 5 mM $MgCl_2$ (A) ATP binding in the absence of 2-ketoglutarate. (B) ATP binding in the presence of 1 mM 2-ketoglutarate. (C) ADP binding to PII. In the sensorgrams, experimental curves are shown in gray and the fitting curves are shown in black.

dissociation rate constant of PII–ADP complex was 1.21-folds significantly lower than that of PII–ATP. In general larger difference in the binding of ATP and ADP was observed primarily in association rates compared to the dissociation rates.

Isothermal titration calorimetry

ITC study was used in order to complement the results obtained from SPR study. Purified recombinant Mtb PII (12–15 µM) was titrated with ATP and ADP. The results of the thermodynamic quantities governing the binding of ATP and ADP are displayed in Table 2 and

Table 1. Dissociation and association rate constants and equilibrium dissociation constants of nucleotides binding to PII protein.

Binding molecule	SPR			ITC
	k_a ($M^{-1}s^{-1}$)	k_d (s^{-1})	K_d (μM)[a]	K_d (μM)
ATP	512 ± 21.6	$(9.85 \pm 0.15) \times 10^{-4}$	1.93 ± 0.08	6.44 ± 1.36
ATP (1 mM 2-ketoglutarate)	309 ± 10.7	$(5.70 \pm 0.10) \times 10^{-4}$	1.84 ± 0.06	8.87 ± 2.82
ADP	74.8 ± 5.9	$(8.17 \pm 0.10) \times 10^{-4}$	10.97 ± 0.78	29.27 ± 7.82

SPR study was carried out at 25°C and ITC was carried out at 30°C. Errors reported for the k_d and k_a values are the standard errors of fitting calculated by the BIA evaluation 3.1 software. K_d values obtained using ITC correspond to the average of three experiments ± standard deviation. [a]Equilibrium dissociation constants (K_d) for the SPR study were calculated from k_a and k_d values using $K_d = k_d/k_a$.

Table 2. Thermodynamic parameters determined for the binding of nucleotides to PII protein.

Binding molecule	ΔH (kcal/mol)	$T\Delta S$ (kcal/mol)	ΔG (kcal/mol)	Stoichiometry
ATP	-3.18 ± 0.09	3.73 ± 0.30	-7.20 ± 0.13	1.28 ± 0.09
ATP (1 mM 2-ketoglutarate)	-3.48 ± 0.11	3.53 ± 0.27	-7.03 ± 0.21	1.41 ± 0.09
ADP	-2.04 ± 0.60	3.33 ± 0.51	-6.30 ± 0.18	3.21 ± 0.44

ITC was carried out at 30°C. All values are average of three experiments ± standard deviation.

the titration plots are shown in Fig. 3. The upper panels of each interaction data illustrates saturation substrate binding by the Mtb PII protein. It is evident that both the interactions were exothermic. The data were fitted to one-site binding model (Table 2). Results of the Welch 2 sample *t*-tests for assessing the significance of difference between the means of triplicate experiments of thermodynamic quantities governing binding of ATP and ADP to Mtb PII are displayed in Supplementary Table S1.

ATP bound to Mtb PII with high affinity ($K_d = 6.44 \pm 1.36$ μM). The binding of ATP to Mtb PII resulted from favourable contribution from binding enthalpy ($\Delta H = -3.18 \pm 0.09$ kcal/mol) and entropy ($T\Delta S = 3.73 \pm 0.30$ kcal/mol). ITC data suggested a stoichiometry of 1.28 ± 0.09 molecules of ATP per Mtb PII monomer suggesting one molecule of ATP for each Mtb PII monomer. The stoichiometry of the interaction between PII and ADP was 3.21 ± 0.44. The binding affinity of PII to ADP is low as found by both SPR and ITC studies. It is known that in cases of weak binding, the value of *N* (stoichiometry) is not well determined by the shape of the ITC titration curve and may float unrealistically during ITC fitting (ITC notes, Alan Cooper, University of Glasgow). Therefore, the binding stoichiometry value of 3.21 is not reflecting the true stoichiometry of the binding of ADP to PII and is actually a consequence of non-specific interaction of ADP molecules with PII, possibly at positions other than the nucleotide-binding pocket.

We next investigated the effect of 2-ketoglutarate on the binding of ATP to Mtb PII. In the presence of 1 mM 2-ketoglutarate, the dissociation constant of Mtb PII for ATP (8.87 ± 2.82 μM) was not significantly different from the dissociation constant of Mtb PII for ATP in the absence of 2-ketoglutarate. The binding exothermic enthalpy of binding of ATP to Mtb PII in presence of 2-ketoglutarate was significantly different and lower ($P < 0.05$) from that in the absence of 2-ketoglutarate (Supplementary Table S1). These results indicate an enhancing influence of 2-ketoglutarate on the binding enthalpy of ATP to Mtb PII. However, the entropy and free energy of binding for these two cases were not significantly different. It is believed that the thermodynamic equation of $\Delta G = \Delta H - T\Delta S$ is not violated here. However, statistically significant changes in the corresponding ΔG and ΔS values were not observed perhaps due to variability among the replicate experiments beyond our control.

In order to examine the substrate specificity of Mtb PII, we measured the thermodynamic parameters for binding of Mtb PII with ADP. The experiment supported the SPR findings and showed that Mtb PII binds to ADP with significantly lower affinity compared to ATP. The binding exothermic enthalpy of Mtb PII with ADP was also significantly lower than that of ATP binding to Mtb PII (Table 2, Supplementary Table S1).

Comparison of the results obtained from SPR and ITC experiments revealed that although the dissociation constants are in the same order but they differ by ~1–4-folds depending on the substrates. This difference may be attributed to the differences in the type of assay. Depending on thermodynamic and diffusion properties, the immobilization of proteins to a solid phase matrix in the case of SPR, can theoretically affect rate constants by 2–10-fold compared with solution measurements (*37*). Also, the slight change in Mtb PII conformation at 25 and 30°C, as indicated by change in CD signal, could underlie the minor differences found in the dissociation constants between ITC and SPR experiments although they are of the same order.

ATP and 2-Ketoglutarate Docking Study

Recently the high-resolution (1.4 Å) crystal structure of Mtb PII was deposited in Protein Data Bank (*23*). The X-ray crystal structures of PII from various species showed that all share a highly conserved

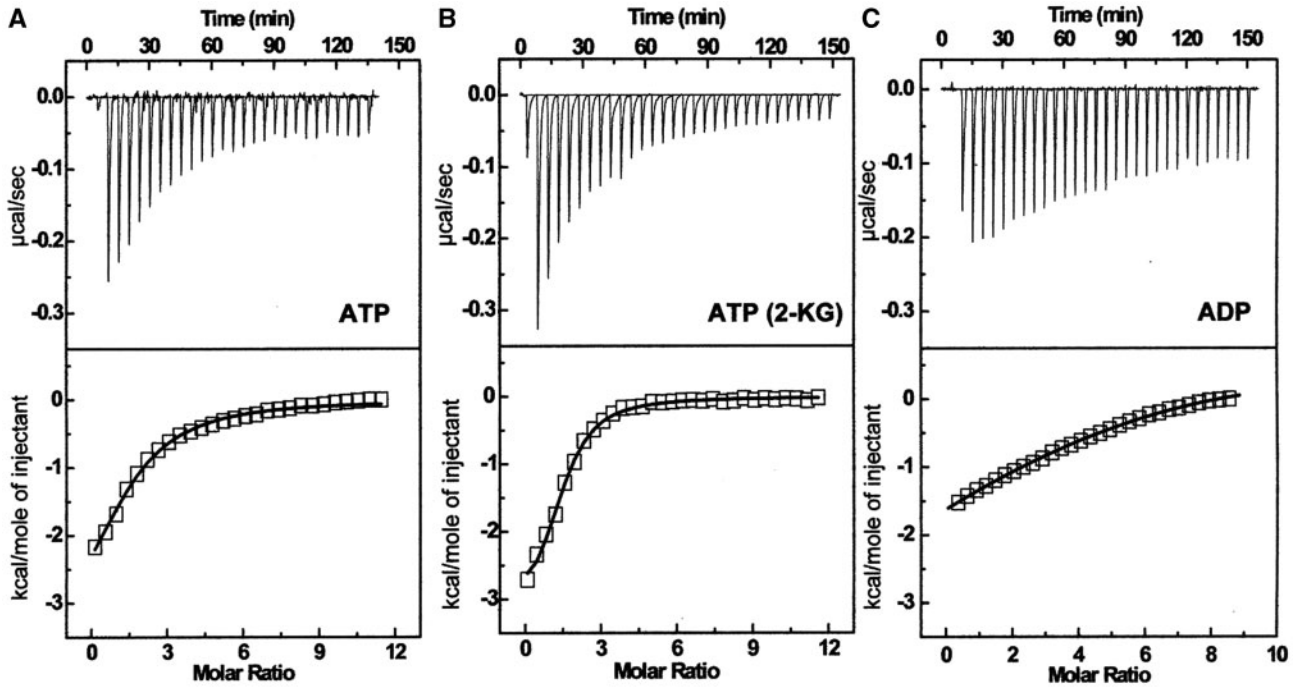

Fig. 3 Binding of nucleotides to Mtb PII studied by isothermal titration calorimetry. (A) ATP binding in the absence of 2-ketoglutarate. (B) ATP binding in the presence of 1 mM 2-ketoglutarate. (C) ADP binding to PII. Experiments were carried out in the presence of 5 mM $MgCl_2$ in triplicates. All titrations were performed at 30°C using a syringe while stirring continuously at 300 rpm. For determination of binding isotherms, the protein solution (12–15 µM protein in ITC buffer) was titrated with 15–30 additions of nucleotide solution (5 µl of 1 mM each). Each injection of nucleotide lasted 5 s with 5 min interval between successive injections. The *upper panels* of each part show the raw titration data obtained for injections of the nucleotides into the protein solution and the *lower panels* show the integrated areas for the peaks normalized to the nucleotide/protein molar ratio.

monomer structure arranged into a tightly associated trimer (*38–45*). We used Mtb PII crystal structure in order to understand the bonding interactions of ATP and 2-ketoglutarate and ADP (Fig. 4A–D). Each ATP molecule forms hydrogen bonds with R101, R103 and L112 of one monomer and with K58, G87, G89 and K90 of the adjacent monomer (Fig. 4A). The hydrogen bonding pattern is listed in Table 3.

The structure of PII protein from *Methanococcus jannaschii* (PDB id 2J9E) showed the binding of 2-ketoglutarate to the T-loop region in one of the chains of the homotrimer. Of all known crystal structures of PII, this is the first structure solved with the binding of 2-ketoglutarate and ATP. The loop of the *M. jannaschii* PII protein (*29*) had a different conformation from that in Mtb PII structure 3BZQ. We therefore used the *M. jannaschii* PII protein structure as the template to model the binding of 2-ketoglutarate to Mtb PII assuming similar binding characteristics (Fig. 4C). We predicted that 2-ketoglutarate binds to the bended T-loop of Mtb PII. Residues E50, S52, V53 and D54 form hydrogen bonds with 2-ketoglutarate molecule (Fig. 4B). The modified loop conformation raises the possibility of formation of additional hydrogen bonds between γ-phosphate of ATP and residues Glycine 37 (G37) and Arginine 38 (R38) of PII (Fig. 4D). ADP molecule lacks γ-phosphate but it is present in ATP molecule.

Glutaraldehyde crosslinking reaction

Glutaraldehyde crosslinking experiments were performed in order to examine the oligomer forms of Mtb PII protein. Our attempts to examine the oligomers of PII using purified N-terminal his-tagged protein did not reveal clear results. Therefore we attempted to examine this phenomenon using C-terminal his-tag purified protein. We observed that the Mtb PII-C protein formed specific and stable trimers on incubation with glutaraldehyde. The molecular weight of Mtb PII-C protein along with the C-terminal his-tag was calculated as 15.2 kDa. Therefore, the oligomeric structure of Mtb PII-C is suggested to be a homotrimer of ~45.6 kDa (Fig. 5). This finding is in agreement with other bacterial and eukaryotic PII proteins (*3*). In order to ensure that the results obtained from Mtb PII-C crosslinking was due to specific protein self association and not due to non-specific crosslinking, a wide range of protein to glutaraldehyde ratios were checked. Even at high glutaraldehyde concentrations the trimeric form of the protein was most prevalent and no higher structure formation was evident. This indicated the specificity of the cross-linking reaction. The negative control was Mtb PII-C incubated under the same conditions without glutaraldehyde.

Molecular Phylogenetic Analysis

We aimed to compare the mycobacterial PII proteins with the PII proteins of Proteobacteria (Fig. 6). The phylogenetic trees of PII proteins were inferred from the distance matrix analysis. In *M. tuberculosis*, there are two inferences, namely that the PII could be either a GlnB homolog or a GlnK homolog. Therefore, two phylogenetic trees were generated: one comparing the

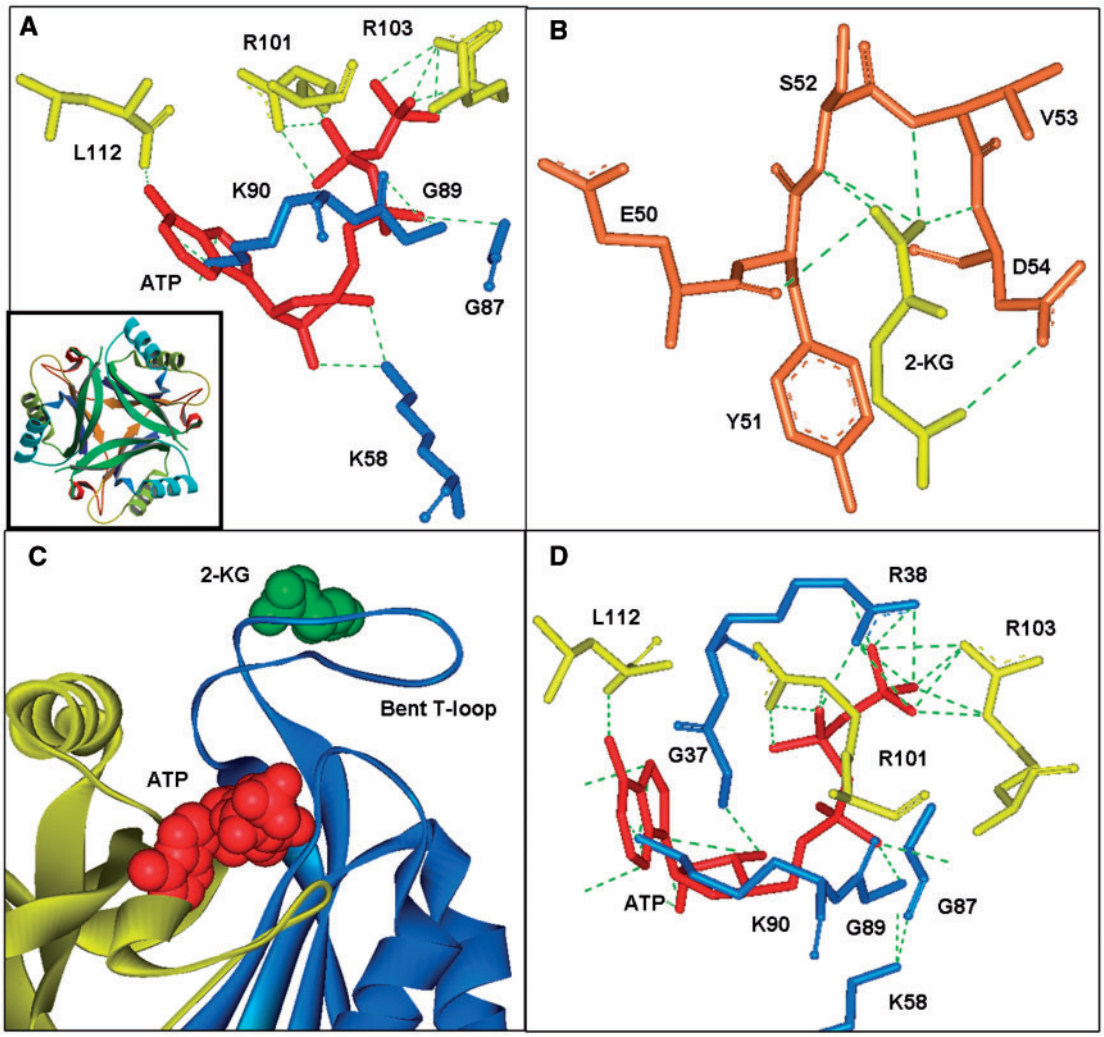

Fig. 4 Docking of ATP and 2-ketoglutarate on PII crystal structure (PDB id 3BZQ). (A) ATP molecule positioned in the lateral cleft and the side chains of neighbouring amino acid residues. R101, R103 and L112 residues are from chain A (yellow) of the trimer; K58, G89 and K90 residues are from chain B (blue). This binding is in the absence of 2-ketoglutarate. The inset shows the 3D structure of Mtb PII (PDB id-3BZQ) in the trimeric state (B) Location of 2-ketoglutarate (2-KG) on the bended T-loop. The 2-ketoglutarate molecule forms hydrogen bonds with Glu50 (E50), Ser52 (S52), Val53 (V53) and Asp54 (D54). (C) ATP molecule docked in the presence of 2-ketoglutarate molecule and the bent T-loop (D) ATP molecule positioned in the lateral cleft forms hydrogen bonds with Arg38 (R38) and Gly37 (G37) present on the bent T-loop of PII in the presence of 2-ketoglutarate. Hydrogen bonds are shown as green dotted lines.

actinobacterial PII with the GlnB genes from proteobacteria (Fig. 6B) and the other tree comparing actinobacterial PII with GlnK genes from proteobacteria (Fig. 6C). Both the trees were unrooted. The topologies of the trees imply that the PII proteins from actinobacteria form a lineage distinct from both GlnK and GlnB lineages of proteobacteria. Multiple alignments using ClustalW (*31*) with default parameters showed that residues forming the T-loop including Tyr-51 (site for post-translational modification) and the ATP-binding site are conserved (Supplementary Figure S2 and S3). The actinobacterial lineage includes experimentally characterized GlnK from *S. coelicolor* and *C. glutamicum*, and to our knowledge the Mtb PII (recombinant Rv2919c) protein is the first mycobacterial PII to be experimentally characterized and reported in this work. The Rv2919c PII formed a common clade with the other mycobacterial PII proteins and consistently grouped with the PII proteins from other actinobacteria. The *M. tuberculosis* and *M. bovis* PII sequences are 100% identical and therefore do not resolve into separate branches. The Rv2919c PII with 98% sequence identity to *M. avium* separates as a short branch. The saprophytic mycobacterium *M. smegmatis* with 88% identity, diverges from these three species mycobacteria (*M. tuberculosis* H37Rv, *M. bovis*, *M. avium*). The phylogenetic trees inferred from GlnB and GlnK separately showed that in both the cases proteobacterial GlnB and GlnK formed lineages distinct and distant from the actinobacterial lineage.

Discussion

In this study, we aimed to clone, express and purify PII protein of *M. tuberculosis* and characterize its molecular properties and phylogenetic relationship. We identified the ATP-binding property of Mtb PII. SPR and

Table 3. Hydrogen bonding pattern of Mtb PII with ATP and 2-ketoglutarate.

H-bond formed between	PII residues involved in H-bonding	Ligand atoms involved in H-bonding
2-Ketoglutarate (2-KG) and PII C-chain	GLU50: O	2-KG: O1
	SER52: N	2-KG: O1
	SER52: N	2-KG: O2
	VAL53: N	2-KG: O2
	ASP54: N	2-KG: O2
	ASP54: OD2	2-KG: O4
ATP and PII (in the absence of 2-ketoglutarate bound to T-loop of PII C-chain)	*PII B-chain*	
	ARG101: NH1	ATP: O2B
	ARG101: NH1	ATP: O1B
	ARG101: NE	ATP: O1B
	ARG103: NH2	ATP: O1G
	ARG103: NH2	ATP: O2G
	ARG103: NH2	ATP: O3G
	ARG103: NE	ATP: O2G
	ARG103: NE	ATP: O3G
	LEU112: OXT	ATP: N6
	PII C-chain	
	LYS58: NZ	ATP: O2′
	LYS58: NZ	ATP: O3′
	GLY89: O	ATP: O1A
	GLY89: N	ATP: O1A
	LYS90: NZ	ATP: N1
	LYS90: NZ	ATP: N3
	LYS90: NZ	ATP: N7
ATP and PII (in the presence of 2-ketoglutarate bound to T-loop of PII C-chain)	*PII B-chain*	
	ARG101: NH1	ATP: O2B
	ARG101: NH1	ATP: O1B
	ARG101: NE	ATP: O1B
	ARG103: NH2	ATP: O1G
	ARG103: NH2	ATP: O2G
	ARG103: NH2	ATP: O3G
	ARG103: NE	ATP: O2G
	ARG103: NE	ATP: O3G
	LEU112: OXT	ATP: N6
	PII C-chain	
	TYR36: N	ATP: O2′
	TYR36: O	ATP: O2′
	TYR36: O	ATP: O3′
	GLY37: N	ATP: O3′
	ARG38: NH1	ATP: O1B
	ARG38: NH1	ATP: O1G
	ARG38: NH1	ATP: O2G
	ARG38: NH2	ATP: O1G
	ARG38: NH2	ATP: O3G
	ARG38: NE	ATP: O1G
	GLY89: O	ATP: O1A
	GLY89: N	ATP: O1A
	LYS90: NZ	ATP: N1
	LYS90: NZ	ATP: N3
	LYS90: NZ	ATP: N7

N: Nitrogen, H: Hydrogen, O: Oxygen, A: Alpha, B: Beta, G: Gamma, D: Delta, E: Epsilon, Z: Zeta.

ITC measurements clearly demonstrated that Mtb PII is an ATP-binding protein. The binding of *E. coli* PII ($K_d = 1.49 \pm 0.08\,\mu M$) (*7*) and of Mtb PII binding to ATP were observed to be of same order. The Mtb PII also binds to ADP but with an order of lower affinity. The binding of *A. thaliana* PII to ADP has been previously reported ($K_d = 69.9 \pm 12.1\,\mu M$) (*5*) and this binding is of the same order as Mtb PII. Our study of association and dissociation rate constants using SPR revealed that the relative difference in the binding affinities of ATP and ADP to Mtb PII is mainly due to the large difference in their association rates while the dissociation rate constants had comparatively smaller difference (Table 1). The binding of ADP to Mtb PII is weaker compared to ATP because Mtb PII–ATP binding involves an elaborate hydrogen bonding network from oxygen atoms of ATP as shown by the ATP docking study (Fig. 4A). ATP forms hydrogen bonds with Arg103 through its γ-phosphate; therefore, absence of γ-phosphate could perhaps underlie the lower affinity of Mtb PII for ADP.

Biochemical studies on *E. coli* PII and ITC studies on *A. thaliana* PII have shown enhanced binding of ATP in the presence of 2-ketoglutarate (4.5–6-fold increase in affinity) (*5*, *7*). No such observation has so far been reported from experimentally studied actinobacterial PII proteins (*15–17*). In case of Mtb PII, both ITC and SPR study showed that there was no significant difference in the binding affinity of ATP to Mtb PII either in the presence or in the absence of high levels of 2-ketoglutarate. However, significant differences were observed in the binding enthalpies in the ITC experiments.

A multiple sequence alignment analysis of crystallized PII protein sequences using ClustalW (*31*) showed that the T-loop sequence is well conserved (Supplementary Figure S4). Forty-six percent residues constituting the T-loop were identical in all sequences, 17% residues have conserved substitution and 4% residues showed semiconserved substitution. The T-loop has a highly flexible conformation and therefore has been predicted to play a pivotal role in interaction with other proteins such as the ammonium transporter AmtB and NAGK (*N*-acetyl-L-glutamate kinase) (*3*, *46*, *47*). Prediction of disordered conformation (*48–50*) of the T-loop sequences of crystallized PII proteins showed that the entire stretch of sequences are likely disordered in all except in the case of *Methanococcus jannaschii* wherein the prediction values are very close to the threshold values (Supplementary Table S2). This prediction is in agreement with the observed crystal structure in all cases known so far. This finding indicates a strong selective pressure for maintaining the structural flexibility of T-loop by keeping its amino acid sequence conserved to maintain disordered state of conformation. Co-crystallization studies with *E. coli* GlnK and AmtB showed that the interaction between these two proteins occurs through the T-loop of GlnK (*46*). More recently, co-crystallization of PII with NAGK (*N*-acetyl-L-glutamate kinase) of *Synechococcus elongatus* strain PCC7942, emphasized on the key role played by T-loop of PII protein in protein–protein interactions (*47*). These observations show that the conservation of the T-loop sequence and its disordered state allows interaction with small molecules (e.g. 2-ketoglutarate) and other proteins. This property is in agreement with known characteristics of disordered regions exhibiting propensity for multiple interactions (*51*).

Previous reports suggesting the probable binding site of 2-ketoglutarate molecule were based on indirect evidences. Structural alignment study of *H. seropedicae* PII with other α-keto-acid-binding proteins and

mutagenesis study in *E. coli* suggested the lateral cleft as the 2-ketoglutarate-binding site (*40*, *52*). The crystal structure analysis of *E. coli* GlnK/ATP complex predicted the T-loop as the probable binding site for 2-ketoglutarate (*38*). In the recently published structure of *Methanococcus jannaschii* PII protein (2J9E), it is evident that 2-ketoglutarate binds to the T-loop and interacts with residues 52–54. The structure of T-loop in complex with the 2-ketoglutarate is considerably different from the unbound T-loop structure. We used this crystal structure as template to model the interaction of 2-ketoglutarate with Mtb PII. It was observed that during the bending of the T-loop and binding to 2-ketoglutarate, additional hydrogen bond formations are possible between ATP and residues of the PII peptide chain (Gly37 and Arg38). These additional hydrogen bonds may underlie the increased exothermic enthalpy of PII–ATP binding in the presence of 2-ketoglutarate observed in our experiments. Crosslinking experiments show that Mtb PII also exists in trimeric form as has been observed with other PII orthologues (*3*, *5*).

In summary, our analysis of the biochemical properties of Mtb PII showed that it conforms to the basic characteristics of other PII orthologues. The significance of the disordered region in PII in terms of allowing flexibility to interact with other proteins, post-translational modification and increased hydrogen bond formations through small molecule binding (e.g. 2-ketoglutarate) are noteworthy.

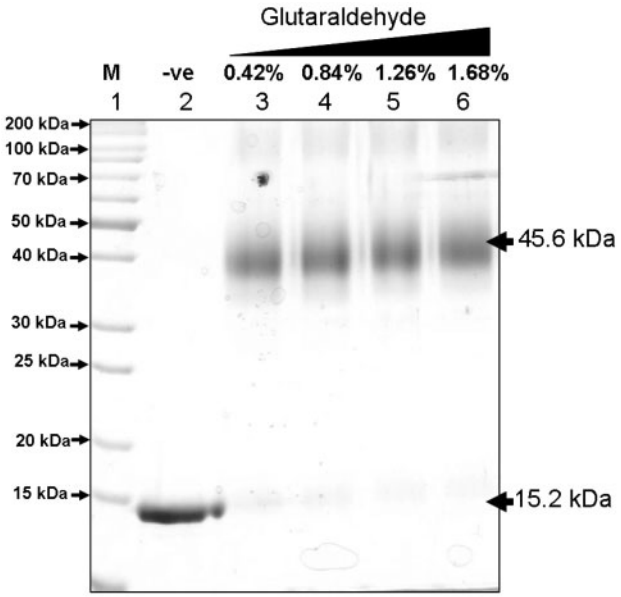

Fig. 5 Mtb PII is a trimer. Purified Mtb PII-C incubated with increasing concentrations of the amino group specific crosslinker glutaraldehyde for 4 h at 37°C. After stopping the reaction samples were electrophoresed on a 12% SDS–PAGE. Lane 1: molecular weight marker, lane 2: PII-C with no glutaraldehyde, lane 3: 0.42% glutaraldehyde, lane 4: 0.84% glutaraldehyde, lane 5: 1.26% glutaraldehyde, lane 6: 1.68% glutaraldehyde.

Supplementary Data

Supplementary Data are available at *JB* online.

Acknowledgements

A.B. and S.R. thank Dr Somdutta Sen for help with mass spectrometric analysis. S.R. thanks Dr Bhupesh Taneja for advice on calculating inter-atom distances, Raghunandan for systems support and Ms Jyotasana Gulati for help with docking study. We thank Mr Gajender Saini (System Analyst) of Advanced Instrumentation Research Facility (AIRF), Jawaharlal Nehru University (JNU) for providing technical help in Circular Dichroism experiment.

Funding

A.B. and S.J. are recipients of research fellowship from Council of Scientific and Industrial Research (CSIR) and University Grants

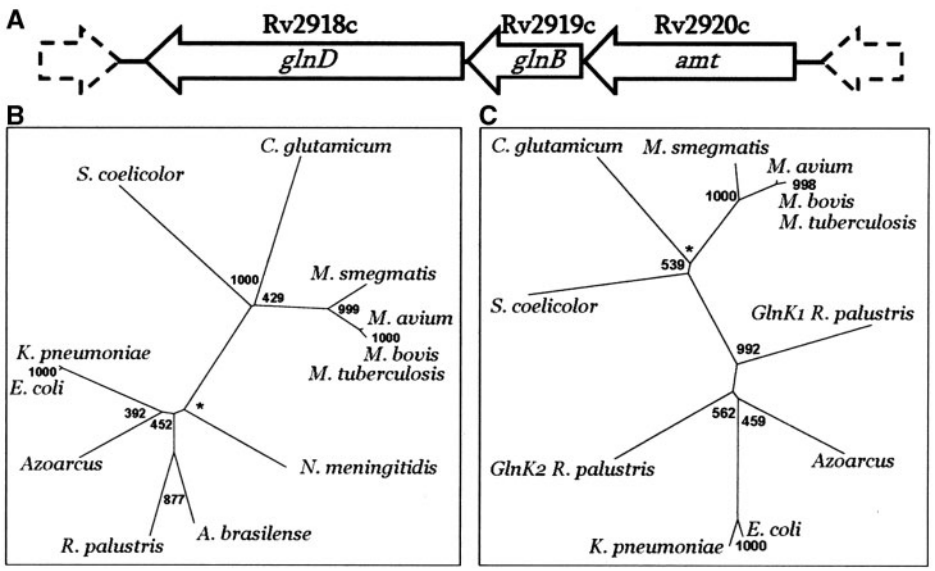

Fig. 6 PII phylogenetic tree. (A) Genomic location of the coding region of *Rv2919c* PII (*glnB* or *glnK*). (B) Phylogenetic tree of PII proteins from actinomycetes and GlnB proteins from proteobacteria. (C) Phylogenetic tree of PII proteins from actinomycetes and GlnK proteins from proteobacteria. Note that the actinomycete lineage is distinct from both GlnB and GlnK lineages of proteobacteria. Asterisks indicate the bootstrap values are inconsistent for the particular branch points.

Commission (UGC); grants 'Molecular biology of Pathogens SMM0003' and '*In silico* biology for drug target identification CMM0017' from CSIR and a travel grant under Indo-Russia cooperation to S.R.; Russian Foundation for Basic Research (Project No. 05-04-49283) to V.A.I., E.S.F. and S.S.P.).

Conflict of interest
None declared.

References

1. Zhang, Y. (2005) The magic bullets and tuberculosis drug targets. *Annu. Rev. Pharmacol. Toxicol.* **45**, 529–564
2. Skeiky, Y.A. and Sadoff, J.C. (2006) Advances in tuberculosis vaccine strategies. *Nat. Rev. Microbiol.* **4**, 469–476
3. Arcondeguy, T., Jack, R., and Merrick, M. (2001) P(II) signal transduction proteins, pivotal players in microbial nitrogen control. *Microbiol. Mol. Biol. Rev.* **65**, 80–105
4. Ninfa, A.J. and Atkinson, M.R. (2000) PII signal transduction proteins. *Trends Microbiol.* **8**, 172–179
5. Smith, C.S., Weljie, A.M., and Moorhead, G.B. (2003) Molecular properties of the putative nitrogen sensor PII from *Arabidopsis thaliana*. *Plant J.* **33**, 353–360
6. Jiang, P., Peliska, J.A., and Ninfa, A.J. (1998) Enzymological characterization of the signal-transducing uridylyltransferase/uridylyl-removing enzyme (EC 2.7.7.59) of *Escherichia coli* and its interaction with the PII protein. *Biochemistry*. **37**, 12782–12794
7. Kamberov, E.S., Atkinson, M.R., and Ninfa, A.J. (1995) The *Escherichia coli* PII signal transduction protein is activated upon binding 2-ketoglutarate and ATP. *J. Biol. Chem.* **270**, 17797–17807
8. Jiang, P., Peliska, J.A., and Ninfa, A.J. (1998) Reconstitution of the signal-transduction bicyclic cascade responsible for the regulation of Ntr gene transcription in *Escherichia coli*. *Biochemistry* **37**, 12795–12801
9. Jiang, P., Peliska, J.A., and Ninfa, A.J. (1998) The regulation of *Escherichia coli* glutamine synthetase revisited: role of 2-ketoglutarate in the regulation of glutamine synthetase adenylylation state. *Biochemistry* **37**, 12802–12810
10. van Heeswijk, W.C., Hoving, S., Molenaar, D., Stegeman, B., Kahn, D., and Westerhoff, H.V. (1996) An alternative PII protein in the regulation of glutamine synthetase in *Escherichia coli*. *Mol. Microbiol.* **21**, 133–146
11. Atkinson, M. and Ninfa, A.J. (1999) Characterization of the GlnK protein of *Escherishia coli*. *Mol. Microbiol.* **32**, 301–313
12. Javelle, A., Severi, E., Thornton, J., and Merrick, M. (2004) Ammonium sensing in *Escherichia coli*. Role of the ammonium transporter AmtB and AmtB-GlnK complex formation. *J. Biol. Chem.* **279**, 8530–8538
13. de Zamaroczy, M. (1998) Structural homologues P(II) and P(Z) of *Azospirillum brasilense* provide intracellular signalling for selective regulation of various nitrogen-dependent functions. *Mol. Microbiol.* **29**, 449–463
14. Martin, D.E., Hurek, T., and Reinhold-Hurek, B. (2000) Occurrence of three PII-like signal transmitter proteins in the diazotrophic proteobacterium *Azoarcus* sp. BH72. *Mol. Microbiol.* **38**, 276–288
15. Teixeira, P.F., Jonsson, A., Frank, M., Wang, H., and Nordlund, S. (2008) Interaction of the signal transduction protein GlnJ with the cellular targets AmtB1, GlnE and GlnD in *Rhodospirillum rubrum*: dependence on manganese, 2-oxoglutarate and the ADP/ATP ratio. *Microbiology* **154**, 2336–2347
16. Cole, S.T., Brosch, R., Parkhill, J., Garnier, T., Churcher, C., Harris, D., Gordon, S.V., Eiglmeier, K., Gas, S., Barry, C.E. 3rd, Tekaia, F., Badcock, K., Basham, D., Brown, D., Chillingworth, T., Connor, R., Davies, R., Devlin, K., Feltwell, T., Gentles, S., Hamlin, N., Holroyd, S., Hornsby, T., Jagels, K., Krogh, A., McLean, J., Moule, S., Murphy, L., Oliver, K., Osborne, J., Quail, M.A., Rajandream, M.A., Rogers, J., Rutter, S., Seeger, K., Skelton, J., Squares, R., Squares, S., Sulston, J.E., Taylor, K., Whitehead, S., and Barrell, B.G. (1998) Deciphering the biology of *Mycobacterium tuberculosis* from the complete genome sequence. *Nature* **393**, 537–544
17. Strosser, J., Ludke, A., Schaffer, S., Kramer, R., and Burkovski, A. (2004) Regulation of GlnK activity: modification, membrane sequestration and proteolysis as regulatory principles in the network of nitrogen control in *Corynebacterium glutamicum*. *Mol. Microbiol.* **54**, 132–147
18. Hesketh, A., Fink, D., Gust, B., Rexer, H.U., Scheel, B., Chater, K., Wohlleben, W., and Engels, A. (2002) The GlnD and GlnK homologues of *Streptomyces coelicolor* A3(2) are functionally dissimilar to their nitrogen regulatory system counterparts from enteric bacteria. *Mol. Microbiol.* **46**, 319–330
19. Cole, S.T. (1999) Learning from the genome sequence of *Mycobacterium tuberculosis* H37Rv. *FEBS Lett.* **452**, 7–10
20. Laemmli, U.K. (1970) Cleavage of structural proteins during the assembly of the head of bacteriophage T4. *Nature* **227**, 680–685
21. Bradford, M.M. (1976) A rapid and sensitive method for the quantitation of microgram quantities of protein utilizing the principle of protein-dye binding. *Anal. Biochem.* **72**, 248–254
22. R Development Core Team (2005) *R: A Language and Environment for Statistical Computing*. R Foundation for Statistical Computing, Vienna, Austria
23. Reddy, M.C.M., Palaninathan, S.K., Shetty, N.D., Owen, J.L., and Sacchettini, J.C. Crystal structure of nitrogen regulatory protein from *Mycobacterium tuberculosis*, In press
24. Ivanisenko, V.A., Pintus, S.S., Grigorovich, D.A., and Kolchanov, N.A. (2005) PDBSite: a database of the 3D structure of protein functional sites. *Nucleic Acids Res.* **33**, D183–D187
25. Ivanisenko, V.A., Pintus, S.S., Grigorovich, D.A., and Kolchanov, N.A. (2004) PDBSiteScan: a program for searching for active, binding and posttranslational modification sites in the 3D structures of proteins. *Nucleic Acids Res.* **32**, W549–W554
26. Fomin, E.S., Alemasov, N.A., Aknazarov, Z.I., Chirtsov, A.S., and Fomin, A.E. (2007) Template library MOLKERN as a framework for building effective molecular modeling programs. *Proceedings of the Third Moscow Conference on Computational Molecular B.biology, MCCMB'07, Moscow, Russia*, 27–31 July 2007. pp. 90–91
27. Morris, G.M., Goodsell, D.S., Halliday, R.S., Huey, R., Hart, W.E., Belew, R.K., and Olson, A.J. (1998) Automated Docking Using a Lamarckian Genetic Algorithm and Empirical Binding Free Energy Function. *J. Comput. Chem.* **19**, 1639–1662
28. Schwede, T., Kopp, J., Guex, N., and Peitsch, M.C. (2003) SWISS-MODEL: An automated protein homology-modeling server. *Nucleic Acids Res.* **31**, 3381–3385

29. Yildiz, O., Kalthoff, C., Raunser, S., and Kuhlbrandt, W. (2007) Structure of GlnK1 with bound effectors indicates regulatory mechanism for ammonia uptake. *EMBO J.* **26**, 589–599
30. Davis, J.C., Venkataraman, G., Shriver, Z., Raj, P.A., and Sasisekharan, R. (1999) Oligomeric self-association of basic fibroblast growth factor in the absence of heparin-like glycosaminoglycans. *Biochem. J.* **341**, 613–620
31. Thompson, J.D., Higgins, D.G., and Gibson, T.J. (1994) CLUSTAL W: improving the sensitivity of progressive multiple sequence alignment through sequence weighting, position specific gap penalties and weight matrix choice. *Nucleic Acids Res.* **22**, 4673–4680
32. Felsenstein, J. (1989) PHYLIP- Phylogeny Inference Package (Version 3.2) *Cladistics* **5**, 164–166
33. Veerassamy, S., Smith, A., and Tillier, E.R. (2003) A transition probability model for amino acid substitutions from blocks. *J. Comput. Biol.* **10**, 997–1010
34. Kidd, K.K. and Sgaramella-Zonta, L.A. (1971) Phylogenetic analysis: concepts and methods. *Am. J. Hum. Genet.* **23**, 235–252
35. Rzhetsky, A. and Nei, M. (1993) Theoretical foundation of the minimum-evolution method of phylogenetic inference. *Mol. Biol. Evol.* **10**, 1073–1095
36. Felsenstein, J. (1985) Confidence limits on phylogenies: an approach using bootstrap. *Evolution* **39**, 783–791
37. Karlsson, R., Roos, H., Fägerstam, L., and Persson, B. (1994) Kinetic and concentration analysis using BIA technology. *Methods* **6**, 99–110
38. Xu, Y., Cheah, E., Carr, P.D., van Heeswijk, W.C., Westerhoff, H.V., Vasudevan, S.G., and Ollis, D.L. (1998) GlnK, a PII-homologue: structure reveals ATP binding site and indicates how the T-loops may be involved in molecular recognition. *J. Mol. Biol.* **282**, 149–165
39. MacPherson, K.H., Xu, Y., Cheah, E., Carr, P.D., van Heeswijk, W.C., Westerhoff, H.V., Luque, E., Vasudevan, S.G., and Ollis, D.L. (1998) Crystallization and preliminary X-ray analysis of *Escherichia coli* GlnK. *Acta Crystallogr. D Biol. Crystallogr.* **54**, 996–998
40. Benelli, E.M., Buck, M., Polikarpov, I., de Souza, E.M., Cruz, L.M., and Pedrosa, F.O. (2002) *Herbaspirillum seropedicae* signal transduction protein PII is structurally similar to the enteric GlnK. *Eur. J. Biochem.* **269**, 3296–3303
41. Sakai, H., Wang, H., Takemoto-Hori, C., Kaminishi, T., Yamaguchi, H., Kamewari, Y., Terada, T., Kuramitsu, S., Shirouzu, M., and Yokoyama, S. (2005) Crystal structures of the signal transducing protein GlnK from *Thermus thermophilus* HB8. *J. Struct. Biol.* **149**, 99–110
42. Carr, P.D., Cheah, E., Suffolk, P.M., Vasudevan, S.G., Dixon, N.E., and Ollis, D.L. (1996) X-ray structure of the signal transduction protein from *Escherichia coli* at 1.9 A. *Acta Crystallogr. D Biol. Crystallogr.* **52**, 93–104
43. Xu, Y., Carr, P.D., Clancy, P., Garcia-Dominguez, M., Forchhammer, K., Florencio, F., Vasudevan, S.G., Tandeau de Marsac, N., and Ollis, D.L. (2003) The structures of the PII proteins from the cyanobacteria *Synechococcus* sp. PCC 7942 and *Synechocystis* sp. PCC 6803. *Acta Crystallogr. D Biol. Crystallogr.* **59**, 2183–2190
44. Schwarzenbacher, R., von Delft, F., Abdubek, P., Ambing, E., Biorac, T., Brinen, L.S., Canaves, J.M., Cambell, J., Chiu, H.J., Dai, X., Deacon, A.M., DiDonato, M., Elsliger, M.A., Eshagi, S., Floyd, R., Godzik, A., Grittini, C., Grzechnik, S.K., Hampton, E., Jaroszewski, L., Karlak, C., Klock, H.E., Koesema, E., Kovarik, J.S., Kreusch, A., Kuhn, P., Lesley, S.A., Levin, I., McMullan, D., McPhillips, T.M., Miller, M.D., Morse, A., Moy, K., Ouyang, J., Page, R., Quijano, K., Robb, A., Spraggon, G., Stevens, R.C., van den Bedem, H., Velasquez, J., Vincent, J., Wang, X., West, B., Wolf, G., Xu, Q., Hodgson, K.O., Wooley, J., and Wilson, I.A. (2004) Crystal structure of a putative PII-like signaling protein (TM0021) from *Thermotoga maritima* at 2.5 A resolution. *Proteins* **54**, 810–813
45. Nichols, C.E., Sainsbury, S., Berrow, N.S., Alderton, D., Saunders, N.J., Stammers, D.K., and Owens, R.J. (2006) Structure of the PII signal transduction protein of *Neisseria meningitidis* at 1.85 Å resolution. *Acta Crystallograph. Sect. F Struct. Biol. Cryst. Commun.* **62**, 494–497
46. Conroy, M.J., Durand, A., Lupo, D., Li, X.D., Bullough, P.A., Winkler, F.K., and Merrick, M. (2007) The crystal structure of the *Escherichia coli* AmtB-GlnK complex reveals how GlnK regulates the ammonia channel. *Proc. Natl. Acad. Sci. USA* **104**, 1213–1218
47. Llacer, J.L., Contreras, A., Forchhammer, K., Marco-Marin, C., Gil-Ortiz, F., Maldonado, R., Fita, I., and Rubio, V. (2007) The crystal structure of the complex of PII and acetylglutamate kinase reveals how PII controls the storage of nitrogen as arginine. *Proc. Natl. Acad. Sci. USA* **104**, 17644–17649
48. Pandey, N., Ganapathi, M., Kumar, K., Dasgupta, D., Das Sutar, S.K., and Dash, D. (2004) Comparative analysis of protein unfoldedness in human housekeeping and non-housekeeping proteins. *Bioinformatics* **20**, 2904–2910
49. Prilusky, J., Felder, C.E., Zeev-Ben-Mordehai, T., Rydberg, E.H., Man, O., Beckmann, J.S., Silman, I., and Sussman, J.L. (2005) FoldIndex: a simple tool to predict whether a given protein sequence is intrinsically unfolded. *Bioinformatics* **21**, 3435–3438
50. Dosztanyi, Z., Csizmok, V., Tompa, P., and Simon, I. (2005) IUPred: web server for the prediction of intrinsically unstructured regions of proteins based on estimated energy content. *Bioinformatics* **21**, 3433–3434
51. Fink, A.L. (2005) Natively infolded proteins. *Curr. Opin. Struct. Biol.* **15**, 35–41
52. Jiang, P., Zucker, P., Atkinson, M.R., Kamberov, E.S., Tirasophon, W., Chandran, P., Schefke, B.R., and Ninfa, A.J. (1997) Structure/function analysis of the PII signal transduction protein of *Escherichia coli*: genetic separation of interactions with protein receptors. *J. Bacteriol.* **179**, 4342–4353